JCTC Journal of Chemical Theory and Computation

Article

pubs.acs.org/JCTC

# Performance of Density Functional Theory for Second Row (4*d*) Transition Metal Thermochemistry

Marie L. Laury and Angela K. Wilson*

Center for Advanced Scientific Computing and Modeling (CASCaM), Department of Chemistry, University of North Texas, Denton, Texas 76203-5017, United States

Supporting Information

**ABSTRACT:** The performances of 22 density functionals, including generalized gradient approximation (GGA), hybrid GGAs, hybrid-meta GGAs, and range-separated and double hybrid functionals, in combination with the correlation consistent basis sets and effective core potentials, have been gauged for the prediction of gas phase enthalpies of formation for the TM-4*d* set, which contains 30 second row transition metal-containing molecules. The enthalpies of formation determined by the 22 density functionals were compared to those generated via the relativistic pseudopotential correlation consistent Composite Approach (rp-ccCA), which has a goal of reproducing energies akin to those from CCSD(T,FC1)-DK/aug-cc-pCV∞Z-DK calculations. B3LYP/cc-pVTZ-PP optimized geometries were used in this study, though structures determined by other functionals also were examined. Of the functionals employed, the double hybrid functionals, B2GP-PLYP and mPW2-PLYP, yielded the best overall results with mean absolute deviations (MADs) from experimental enthalpies of formation of 4.25 and 5.19 kcal mol$^{-1}$, respectively. The GGA functionals BP86 and PBEPBE resulted in deviations from experiment of nearly 100 kcal mol$^{-1}$ for molecules such as molybdenum carbonyls. The ωB97X-D functional, which includes the separation of exchange energy into long-range and short-range contributions and includes a dispersion correction, resulted in an MAD of 6.52 kcal mol$^{-1}$.

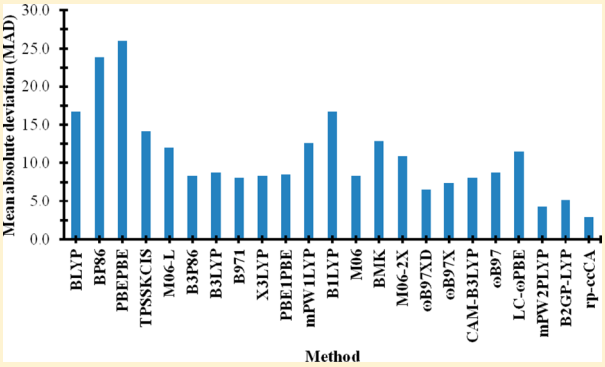


## 1. INTRODUCTION

Density functional theory (DFT) is widely used to study transition metal (TM) molecules since it accounts for electron correlation at a reduced computational cost, as compared to correlated *ab initio* methods. DFT is routinely employed for TM-containing molecules to determine ground state geometries, transition structures, spectroscopic constants, and energetic properties, including bond dissociation energies and enthalpies of formation.[1−7] Through numerous studies of main group species, shortcomings of DFT, such as self-interaction and neglect of long-range effects, have emerged.[8,9] For transition metal species for which functionals are not well (or at all) parametrized, many fewer studies identifying successes and shortcomings of functionals have been done. In fact, there are only a small number of studies that have reported on the shortcomings of some density functionals for 3*d* TM species (see refs 10−13). Among the most severe, and likely most surprising, shortcomings are deviations on the order of 100 kcal mol$^{-1}$ from experimental enthalpies of formation for B3LYP for some 3*d* TMs.[14] While such studies are providing useful insight into methodology needed for 3*d* species, a greater focus upon calibrating functional performance for 4*d* TM species is needed. Benchmark studies of functional performance for 4*d* metal thermochemistry have been limited at best, despite the importance of these species in areas such as catalysis[15] and medicine.[16] Only recently have Truhlar and co-workers examined the performance of DFT for 4*d* atom multiplicities and ionization states.[17]

While DFT is widely employed, *ab initio* calculations are generally preferred for more accurate prediction of energetic properties. For example, for first row transition metals, an *ab initio* composite method, the correlation consistent composite approach (ccCA-TM),[13,18] results in a mean absolute deviation (MAD) of 3 kcal mol$^{-1}$ from experiment for enthalpies of formation ($\Delta H_f$), whereas DFT (e.g. B97-1) has been shown to have errors in excess of 6 kcal mol$^{-1}$ from experimental $\Delta H_f$ values and widely used functionals, such as B3LYP, have deviations of more than 10 kcal mol$^{-1}$ from experiment.[11,19] For main group species, "chemical accuracy" is achieved when thermochemical properties and energies are computed, on average, within 1.0 kcal mol$^{-1}$ of experimental values. While 1.0 kcal mol$^{-1}$ is, in part, physically motivated, there are also a large number of molecules for which the energies from experiment have uncertainties of 1.0 kcal mol$^{-1}$. Thus, 1.0 kcal mol$^{-1}$ is a very convenient gauge for calculated properties. Unfortunately, such a convenient gauge is not presently supported by experimental data (i.e., enthalpies, ionization energies, and

Received: May 9, 2013

   dx.doi.org/10.1021/ct400379z | J. Chem. Theory Comput. XXXX, XXX, XXX−XXX

electron affinities) for transition metals, where the experimental uncertainties, on average, are much larger. Instead, a useful gauge, as suggested in prior work,[20] is the average of the experimental uncertainties. In this earlier work, 3.0 kcal $mol^{-1}$ was suggested as a gauge of theoretical methods and was coined as "transition metal chemical accuracy", based upon the average uncertainty of a set of over 200 of the best experimentally known thermochemical energies of small transition metal species.

In considering second row transition metals, high accuracy, *ab initio* methods such as CCSD(T) are preferred, but the method scales as $N^7$ where N is the number of basis functions. To reliably model second row transition metals, a larger number of basis functions are needed in comparison to main group elements. Due to the number of basis functions necessary for all-electron calculations of second row transition metals, CCSD(T) is computationally expensive, in terms of memory, disk space, and computer processing time, for second row transition metals. To mitigate the computational cost associated with the 4*d* elements, pseudopotentials or effective core potentials (ECPs) may be employed with valence basis sets, in place of all-electron basis sets. The complicated nodal structure of the valence electrons in the vicinity of the core electrons is replaced with a smooth potential; furthermore, ECPs reduce the number of basis functions necessary for a relativistic description of an atom.[21] Relativistic effects can be incorporated into the ECP, which allows for the use of a nonrelativistic wave function for the valence electrons. In the selection of an ECP, considerations must be made for the size of the core and the fit of the ECP. Generally, small core ECPs, with $(n-1)s^2(n-1)p^6(n)s^n(n-1)d^m$ treated in the valence, are preferred over large core ECPs, where the outermost *s* and *d* electrons in the valence region are treated.[22] The second consideration, fit of the ECP, determines if an ECP is energy- or shape-consistent. Energy-consistent ECPs are fit to atomic valence spectra from all-electron relativistic calculations, while shape-consistent ECPs are designed to match atomic orbital shape.

Recently, the authors developed a relativistic pseudopotential-based composite method, defined as rp-ccCA, and examined the performance of the method for 4*p* and 4*d* molecules.[23] rp-ccCA combines small core, energy-consistent ECPs and a composite method (ccCA) for second row transition metal thermochemistry, enabling a reduced computational cost as compared to a calculation using CCSD(T,FC1)-DK/aug-cc-pwCV∞Z-DK with spin−orbit corrections added perturbatively and with the intent to mimic its accuracy. Since high-cost CCSD(T,FC1) calculations are generally not practical with large basis sets for second row transition metal systems of increasing size, experimental data was used to calibrate rp-ccCA. First, in earlier work on third-row main group (Ga−Kr) species of the G3/05 set, the performance of rp-ccCA was gauged against experiment, and its performance was found to be in good agreement with ccCA, but with one-third reduction in its computational demands. rp-ccCA was then employed in TM studies, and for TM rp-ccCA work, a molecule set composed of 30 $\Delta H_f$ values of 4*d* TM-containing molecules was defined, called TM-4*d*.[23] This set is composed of TM halides, oxides, hydrides, carbides, dimers, and carbonyls, as well as open and closed shell molecules. Selection for inclusion in this set was based upon the availability of reliable experimental data, that is, with small experimental uncertainties. For the TM-4*d* set, rp-ccCA resulted in enthalpies of formation with deviations less than the corresponding experimental uncertainties. In the current study, the TM-4*d* set and rp-ccCA will be utilized to provide comparison for DFT performance.

The density functionals considered in the current study were selected based on their prior successes in benchmark or applied studies of 3*d* and 4*d* TM species. The selected density functionals include third, fourth, and fifth rung functionals. Perdew introduced the "Jacob's ladder of density functionals", where each rung of the ladder represents a different class of functionals.[24] Local spin density approximation (LSDA) functionals, considered the first rung of Jacob's ladder, were omitted due to their known overestimation of binding energies.[25] Second rung functionals, generalized gradient approximation (GGA), include a dependence on the spin-density gradients. Improvements for binding energies are observed, but GGA functionals introduce self-interaction errors as a result of an electron interacting with itself.[26,27] The additional variable in the kinetic energy density significantly decreases the amount of self-correlation in a functional, generally resulting in an increase in accuracy. To address the self-exchange problem of DFT, a percentage of Hartree−Fock (HF) exchange can be integrated into the functional. The resulting functional is referred to as hybrid and is a fourth rung functional.[28] The final rung of Jacob's ladder consists of double-hybrid functionals, where correlation from second-order perturbation theory is added to the correlation functional.[29,30] Additional variants of functionals are available, including range-separated,[31] long-range corrected,[32] and dispersion-corrected functionals,[33] in order to address known shortcomings of DFT, including overestimation of the exchange energy and a poor description of van der Waals interactions.[8] For this work, a broad range of functionals encompassing these various functional categories have been included. Though most functionals do not include transition metal data within their parametrization sets, there are a few density functionals that include transition metals within the parametrization of the functional (e.g., the TMAE9/05 set of 9 atomization energies of metal diatomics, MLBE21/05 of 21 metal−ligand bond energies, 3*d*TMRE18/06 of 18 reaction energies, and MAEE5 of 5 metal atom excitation energies).[4] These functionals include M06 and M06-2X, and they are included within the current study.

In a recent study by Truhlar and Luo, the multiplicities and ionization states of 4*d* TM atoms were examined with a variety of density functionals.[17] The occupancies of the 4*d* and 5*s* orbitals, as determined by DFT, were used in the Truhlar study as one of the measurements of error for functional performance. Overall, it was observed that GGA functionals favored filling the 4*d* orbitals before the 5*s* orbitals, while Hartree−Fock favored filling the 5*s* orbitals before the 4*d* orbitals. The observation about the order of orbital occupation via GGA functionals is counter to what is reported experimentally. In order to fill the 4*d* and 5*s* orbitals in agreement with experiment, a percentage of HF exchange must be introduced to the GGA functional; that is, HGGAs must be employed. Since the percentage of HF exchange is important for the proper description of the 4*d* and 5*s* atomic orbital occupation, it is of interest to examine the role that percentage of HF exchange has on the accuracy of 4*d* transition metal thermochemistry and to consider the utility of different classes of functionals, such as those including perturbation theory

second-order (PT2) correlation and HF exchange, for 4*d* molecules.

In this study, the performance of a variety of density functionals in conjunction with small core ECPs and correlation consistent basis sets is gauged for the prediction of 4*d* TM thermochemistry. The TM-4*d* set of 4*d* $\Delta H_f$ values was utilized to compare the DFT results to those previously obtained with rp-ccCA.[23]

## 2. METHODOLOGY

All DFT calculations were carried out with the GAUSSIAN 09 software package.[34] The small core, energy-consistent relativistic pseudopotentials and the corresponding valence correlation consistent basis sets of triple- and quadruple-$\zeta$ quality were employed.[35] For each molecule in the TM-4*d* set (see Table 1), B3LYP/cc-pVTZ-PP optimized geometries were utilized for single-point energy calculations for each functional. The molecular $\Delta H_f$ values were determined with the cc-pVQZ-PP basis set. It should be noted that enthalpies of formation when determined with both cc-pVTZ and cc-pVQZ for one functional of each type (i.e., BLYP, B3LYP, $\omega$B97XD, and mPW2-PLYP), the cc-pVQZ basis set outperformed the cc-pVTZ basis set by 0.5 kcal mol$^{-1}$, on average; therefore, the cc-pVQZ basis set is utilized throughout this work. Twenty-two functionals were considered, including GGAs (BLYP,[28,36,37] BP86,[38] TPSSKCIS,[39−43] PBEPBE,[44,45] M06-L[46]), hybrid (B3LYP,[28] B97-1,[47] PBE1PBE,[48] B3P86,[49−53] X3LYP,[54] mPW1LYP,[55] B1LYP,[56] BMK,[57] M06, and M06-2X[4]), range-separated ($\omega$B97 and $\omega$B97X,[32] $\omega$B97XD,[58] CAM-B3LYP,[31] LC-$\omega$PBE[59−61]), and double hybrid functionals (B2GP-PLYP,[62] mPW2-PLYP[30]). The list of functionals by type, including percentage HF exchange, percentage PT2 correlation, and the value of the range-separation parameter for the pertinent functionals, is summarized in Table 2. An unrestricted Hartree−Fock (UHF) reference was utilized for open shell calculations. Fine grids were employed for all calculations. These grids include 75 radials shells with 302 angular points per shell (approximately 7000 points per atom). Enthalpies of formation were calculated via the atomization energy approach; that is, the bonds of the ground state molecule are broken homolytically, and the products are the molecule's constituent ground state atoms.[63] Experimental data was used for the atomic enthalpies of formation.[64] The atomic enthalpies of formation are included in the Supporting Information. Similar to the rp-ccCA study, experimental atomic spin−orbit coupling values were included in the atomic energies for the determination of the molecular enthalpies of formation.[67] The experimental ground state configurations were utilized for the atoms. Zero-point energies were scaled by the appropriate scaling factor for each functional as determined in previous work by the authors.[65]

**Table 1. TM-4*d* Molecule Set**

| molecule | ground state | molecule | ground state |
|---|---|---|---|
| YO | $^2\Sigma^+$ | $MoF_2$ | $^5B_2$ |
| ZrO | $^1\Sigma^+$ | $MoF_6$ | $^1A_{1g}$ |
| $ZrO_2$ | $^1A_1$ | $Mo(CO)_5$ | $^1A_1$ |
| ZrCl | $^2\Delta$ | $Mo(CO)_6$ | $^1A_1$ |
| $ZrCl_2$ | $^3\Delta$ | $RuO_4$ | $^1A_1$ |
| $ZrCl_4$ | $^1A_1$ | RhC | $^2\Sigma^+$ |
| ZrBr | $^2\Delta$ | RhO | $^4\Sigma^-$ |
| $ZrBr_4$ | $^1A_1$ | $RhCl_2$ | $^4\Sigma_g^+$ |
| NbO | $^4\Sigma^-$ | AgH | $^1\Sigma^+$ |
| $NbO_2$ | $^2A_1$ | $Cd_2$ | $^1\Sigma_g^+$ |
| $MoO_2$ | $^3B_1$ | CdH | $^2\Sigma^+$ |
| $MoO_3$ | $^1A_1$ | CdCl | $^2\Sigma^+$ |
| $MoOCl_4$ | $^1A_{1g}$ | $CdCl_2$ | $^1\Sigma_g^+$ |
| $MoO_2Cl_2$ | $^1A_{1g}$ | CdBr | $^2\Sigma^+$ |
| MoF | $^6\Sigma^+$ | $CdBr_2$ | $^1\Sigma_g^+$ |

## 3. RESULTS AND DISCUSSION

**3.1. Overall.** The mean absolute deviation (MAD), mean signed deviation (MSD), root-mean-square deviation (RMSD), and standard deviation ($\sigma$) for the predicted enthalpies of formation of the TM-4*d* set relative to experiment for each functional are reported in Table 3. The double hybrid functional, mPW2-PLYP, yields the lowest MAD of 4.25 kcal mol$^{-1}$ for the TM-4*d* molecule set, which is 1.4 kcal mol$^{-1}$ greater than the MAD obtained with rp-ccCA. Similarly, a lower MAD was obtained by the other double hybrid functional studied, B2GP-PLYP (5.19 kcal mol$^{-1}$). The average experimental uncertainty for the TM-4d molecule set is 3.43 kcal mol$^{-1}$. It should be noted that enthalpies of formation were determined with both cc-pVTZ and cc-pVQZ for one functional of each definition (i.e., BLYP, B3LYP, $\omega$B97XD, and mPW2-PLYP). The cc-pVQZ basis set outperformed the cc-pVTZ basis set by, on average, 0.5 kcal mol$^{-1}$; therefore, the cc-pVQZ basis set is utilized throughout this work. Enthalpies

**Table 2. Twenty-two Functionals Arranged by Type and Parameter Values**

| functional | $\%E_x^{HF}$ | $\%E_c^{PT2}$ | $\omega$ | type[a] | functional | $\%E_x^{HF}$ | $\%E_c^{PT2}$ | $\omega$ | type[a] |
|---|---|---|---|---|---|---|---|---|---|
| BLYP | | | | GGA | B1LYP | 25 | | | HGGA |
| BP86 | | | | GGA | M06 | 27 | | | HGGA |
| PBEPBE | | | | GGA | BMK | 42 | | | HGGA |
| TPSSKCIS | | | | GGA | M06-2X | 54 | | | HGGA |
| M06-L | | | | GGA | $\omega$B97XD | 22.2 | | 0.20 | RSH |
| B3P86 | 20 | | | HGGA | $\omega$B97X | 15.8 | | 0.30 | RSH |
| B3LYP | 20 | | | HGGA | CAM-B3LYP | 20 | | 0.33 | RSH |
| B971 | 21 | | | HGGA | $\omega$B97 | | | 0.40 | RS |
| X3LYP | 21.8 | | | HGGA | LC-$\omega$PBE | | | 0.40 | RS |
| PBE1PBE | 25 | | | HGGA | mPW2-PLYP | 55 | 25 | | DH |
| mPW1LYP | 25 | | | HGGA | B2GP-PLYP | 65 | 36 | | DH |

[a]Generalized Gradient Approximation (GGA), hybrid (H), range-separated (RS), double (D). $\%E_x^{HF}$ is the percentage of HF exchange and $\%E_c^{PT2}$ is the percentage of PT2 correlation.


dx.doi.org/10.1021/ct400379z | J. Chem. Theory Comput. XXXX, XXX, XXX−XXX

Table 3. Mean Absolute Deviations, Mean Signed Deviations, Root Mean Square Deviations, and Standard Deviations from Experiment in kcal mol$^{-1}$ for the TM-4*d* Enthalpies of Formation Determined by DFT[a]

| functional | type | MAD | MSD | RMSD | $\sigma$ | functional | type | MAD | MSD | RMSD | $\sigma$ |
|---|---|---|---|---|---|---|---|---|---|---|---|
| BLYP | GGA | 16.69 | 12.09 | 25.39 | 19.13 | B1LYP | HGGA | 16.71 | −16.37 | 22.43 | 14.96 |
| BP86 | GGA | 23.87 | 22.87 | 37.13 | 28.44 | M06 | HGGA | 8.40 | 2.01 | 10.59 | 6.16 |
| PBEPBE | GGA | 26.03 | 25.07 | 40.32 | 30.80 | BMK | HGGA | 12.86 | −1.28 | 15.76 | 9.10 |
| TPSSKCIS | GGA | 14.15 | 13.31 | 22.74 | 17.80 | M06-2X | HGGA | 10.87 | −8.86 | 14.02 | 8.47 |
| M06-L | GGA | 11.64 | 9.27 | 17.27 | 12.36 | $\omega$B97XD | RSH | 6.52 | 0.04 | 8.71 | 5.78 |
| B3P86 | HGGA | 8.34 | 4.93 | 13.40 | 10.48 | $\omega$B97X | RSH | 7.42 | 3.05 | 10.15 | 6.93 |
| B3LYP | HGGA | 8.74 | −5.81 | 10.53 | 5.93 | CAM-B3LYP | RSH | 8.06 | −5.53 | 10.65 | 6.96 |
| B971 | HGGA | 8.10 | 5.28 | 12.28 | 9.24 | $\omega$B97 | RS | 8.74 | 4.92 | 13.03 | 9.66 |
| X3LYP | HGGA | 8.32 | −5.63 | 9.92 | 5.40 | LC-$\omega$PBE | RS | 11.47 | −4.60 | 14.84 | 9.42 |
| PBE1PBE | HGGA | 8.53 | −5.18 | 11.01 | 6.96 | mPW2-PLYP | DH | 4.25 | −2.21 | 5.67 | 3.76 |
| mPW1LYP | HGGA | 12.61 | −12.08 | 16.87 | 11.20 | B2GP-PLYP | DH | 5.19 | −1.26 | 7.87 | 5.92 |

[a]Geometries obtained with B3LYP/cc-pVTZ-PP. Generalized Gradient Approximation (GGA), hybrid (H), range-separated (RS), double (D).

of formation ($\Delta H_f$), signed deviations, and absolute deviations for each molecule and functional combination are detailed in the Supporting Information.

While the fifth rung functionals, the double hybrids, yielded the smallest deviation in $\Delta H_f$ values, in comparison to experiment, for the TM-4*d* set, the third rung functionals, GGAs, resulted in the largest MADs. BP86 and PBEPBE had MADs of 23.87 and 26.03 kcal mol$^{-1}$. The large MAD was rooted in the carbonyl-containing molecules, five molybdenum molecules ($MoF_6$, $MoO_2$, $MoO_3$, $MoO_2Cl_2$, $MoOCl_4$) and $RuO_4$. The determination of the $\Delta H_f$ values of 3*d* TM carbonyl-containing molecules has previously been shown by Tekarli et al. to result in large deviations from experiment for DFT calculations (e.g., over 50 kcal mol$^{-1}$ for GGAs, over 80 kcal mol$^{-1}$ for MGGAs, and over 40 kcal mol$^{-1}$ for HGGAs)[11] and these deviations are also observed in this work for 4*d* TM carbonyl systems. The enthalpies of formation as determined by rp-ccCA for $Mo(CO)_5$ and $Mo(CO)_6$ deviated by 2.4 and 6.3 kcal mol$^{-1}$, respectively, from experiment.[23] A significant lowering of the deviation, when changing from DFT to rp-ccCA, of the calculated enthalpy of formation from the experimental value signifies the need for high-level methods for the carbonyl-containing molecules. With a higher level of theory, a more accurate description of the $\pi$-back bonding present in the TM-carbonyl systems is obtainable, and in turn, the calculated enthalpy of formation of the TM-carbonyl systems is more accurate.

The previous DFT 4*d* atomic study by Truhlar and Luo reported that the hybrid functionals SOGGA11-X, B1LYP, B3LYP, CAM-B3LYP, BMK, and PW6B95 provide the best comparison with experimental ionization potentials and spin states of the 4*d* atoms.[17] These observations are mirrored in the current study for 4*d* molecular $\Delta H_f$ values; the hybrid functionals, both single and double, with a percentage of HF exchange between 20% and 40% yield the lowest deviations from experimental $\Delta H_f$ values. This percentage of HF exchange for 4*d* thermochemistry is in agreement with the ideal percentage of HF exchange for 3*d* transition metal $\Delta H_f$ values as observed in a previous study by Tekarli et al.[11] Furthermore, the ideal percentage of HF exchange (20−40%) for 4*d* $\Delta H_f$ values is in agreement with observations for 4*d* reaction energies involving C−O bond cleavage.[66]

The overall average experimental uncertainty for the TM-4*d* molecule set is 3.43 kcal mol$^{-1}$. Furthermore, the $\Delta H_f$ values determined via rp-ccCA resulted in an MAD of 2.89 kcal mol$^{-1}$ from experimental $\Delta H_f$ values. Except for RhO and $ZrO_2$, $\Delta H_f$ values from DFT calculations exceed the experimental uncertainty for each molecule. The magnitude in the average DFT deviations from the experimental uncertainties range from 0.30 kcal mol$^{-1}$ for ZrCl to 16.0 kcal mol$^{-1}$ for $MoOCl_4$, and 32.8 kcal mol$^{-1}$ for $RuO_4$. The experimental uncertainty and average DFT deviation are reported for each molecule in Table 4. It should be noted that the $\Delta H_f$ values for these two molecules had the largest experimental uncertainties of 10.0 and 11.0 kcal mol$^{-1}$, respectively. Since previous studies have proven rp-ccCA to be a reliable methodology for second row transition metal thermochemistry, the pseudopotential-based composite method is preferred over DFT for accurate energetic and thermodynamic data.

Table 4. Comparison of the Experimental Uncertainty and the Average DFT Absolute Deviation for Each Molecule in the TM-4*d* Molecule Set[a]

| molecule | avg. DFT deviation | exptl. uncertainty | molecule | avg. DFT deviation | exptl. uncertainty |
|---|---|---|---|---|---|
| YO | 7.3 | 2.5 | $MoF_2$ | 7.5 | 4.0 |
| ZrO | 5.8 | | $MoF_6$ | 26.3 | 2.2 |
| $ZrO_2$ | 9.4 | 11.0 | $Mo(CO)_5$ | 27.8 | 5.0 |
| ZrCl | 6.0 | 5.7 | $Mo(CO)_6$ | 31.4 | 1.1 |
| $ZrCl_2$ | 5.4 | 3.6 | $RuO_4$ | 33.8 | 1.0 |
| $ZrCl_4$ | 9.1 | 0.6 | RhC | 11.5 | 2.3 |
| ZrBr | 7.2 | 0.5 | RhO | 9.0 | 10.0 |
| $ZrBr_4$ | 8.6 | 2.0 | $RhCl_2$ | 9.6 | 3.0 |
| NbO | 8.6 | 5.0 | AgH | 1.5 | |
| $NbO_2$ | 13.0 | 5.0 | $Cd_2$ | 1.0 | |
| $MoO_2$ | 11.5 | 3.0 | CdH | 9.4 | |
| $MoO_3$ | 17.4 | 5.0 | CdCl | 6.3 | |
| $MoOCl_4$ | 17.4 | 1.4 | $CdCl_2$ | 5.0 | 1.1 |
| $MoO_2Cl_2$ | 16.3 | 3.5 | CdBr | 3.5 | |
| MoF | 8.5 | 3.0 | $CdBr_2$ | 4.2 | 1.1 |

[a]Units are in kcal/mol.

**3.2. Generalized Gradient Approximation (GGA) Functionals.** Common outliers for the GGA functionals were $MoCO_5$, $MoCO_6$, $MoF_6$, and $RuO_4$. The BP86 and PBEPBE functionals resulted in significant deviations, near 100 kcal mol$^{-1}$, for these molecules. By excluding the outliers for BP86, PBEPBE, and BLYP, the MADs dropped by nearly 70% to 8.75, 10.18, and 10.60 kcal mol$^{-1}$, respectively. The deviation observed for the outliers of TPSSKCIS and M06-L were nearly half of the deviations seen for BP86, PBEPBE, and BLYP;


dx.doi.org/10.1021/ct400379z | J. Chem. Theory Comput. XXXX, XXX, XXX−XXX

therefore, the drop in the MAD with the exclusion of the outliers was not as drastic (50%) for TPSSKCIS and M06-L, 7.12 and 6.91 kcal mol$^{-1}$, respectively. All of the GGA functionals overestimated the enthalpies of formation by, on average, 15 kcal mol$^{-1}$. Overall, the GGAs yielded an MAD of 18.48 kcal mol$^{-1}$ and an MSD of 16.52 kcal mol$^{-1}$. Since the enthalpies of formation are determined via atomization energies, the overestimation of the enthalpies of formation is in agreement with the known overestimation of the binding energies. As mentioned previously in the paper, the introduction of HF exchange into the GGA formula, as designed by Becke, yields the HGGA functionals, where the HF exchange has been shown to mitigate the overestimation of binding energies.[28]

**3.3. Hybrid GGA Functionals.** Since there were ten hybrid functionals included in the study, the effect that the percentage of Hartree−Fock exchange has on the performance of the functional for the TM-4*d* set was examined. For the hybrid functionals, there was not a trend with respect to the MADs and the percentage of Hartree−Fock exchange. The HGGA functionals obtained an overall MAD of 10.35 kcal mol$^{-1}$ and an MSD of −4.30 kcal mol$^{-1}$.

To describe Becke exchange, there are three commonly employed functionals (B, B1, B3) that vary in the theoretical and experimental data utilized for their fitting. The original Becke exchange functional (B) includes one parameter fit to exact atomic HF data, the B1 exchange functional includes a parameter based on the ratio between HF and DFT exchange, and the B3 exchange functional includes three parameters and is fit to Gaussian-1 thermochemistry. The B3 exchange functional significantly reduces the overall MAD in comparison to the B exchange functional, while the introduction of fitting to DFT exchange (B1) did not improve the overall accuracy of the B1-exchange functionals over the B-exchange functionals. The MADs of B3P86 and B3LYP were 8.3 and 8.7 kcal mol$^{-1}$, respectively, in contrast to 16.7 kcal mol$^{-1}$ of BLYP and B1LYP and 23.9 kcal mol$^{-1}$ of BP86.

While nonlocal Hartree−Fock exchange did not improve the accuracy of the functionals with Becke-type exchange, Hartree−Fock exchange did improve the performance of the PBE functionals; the MAD of PBE1PBE was 8.5 kcal mol$^{-1}$ and 26.0 kcal mol$^{-1}$ for PBEPBE. The lowering of the MADs with the inclusion of HF exchange in the exact functional was also observed for 3*d* transition metal thermochemistry, though the difference between the two functionals (e.g., PBE1KCIS and PBEKCIS) was, on average, 2 kcal mol$^{-1}$.[11] The M06 functional yielded a comparable MAD (8.4 kcal mol$^{-1}$) to PBE1PBE. Doubling the amount of exchange for the M06 functional (i.e. M06-2X) did not improve the performance of the functional for 4*d* enthalpies of formation (MAD of 10.9 kcal mol$^{-1}$). The failure of M06-2X for transition metals, specifically 4*d* transition metals, is consistent with observations from Truhlar and Luo's study of DFT for 4*d* atoms.[17] For the 4*d* $\Delta H_f$ values, the HGGAs with the percentage of Hartree−Fock exchange ranging from 20 to 27% have lower MADs in comparison to the HGGAs with additional HF exchange, with the exception of mPW1LYP and B1LYP; the 4*d* results, with respect to HF exchange, are in agreement with previous results for 3*d* thermochemistry.[11] The outliers for these two HGGAs are the same as the outliers of the GGA functionals excluding $MoF_6$, $MoO_2$, and $RuO_4$; therefore, the inclusion of the additional parameter for HF exchange, even the desired percentage in the twenties, does not necessarily improve the performance of a density functional for second row transition metal thermochemistry. To note, the inclusion of the second order perturbation correlation energy significantly reduces the errors observed, specifically for mPW1LYP (HGGA) versus mPW2PLYP (DHGGA).

**3.4. Range-Separated Functionals.** There are two classes of range-separated functionals that are used to describe the exchange energy. For clarity, these functionals will be referred to as RS and RSH. The first class, RS, has one range parameter, $\omega$, to separate the exchange into a long-range and a short-range contribution where the long-range exchange is described by HF and the short-range exchange is described by DFT. An increase in the $\omega$ value results in a decrease in the short-range contribution of DFT to the exchange; that is, the exchange energy is described by a greater contribution of HF exchange. Examples of these one range parameter functionals include $\omega$B97 and LC-$\omega$PBE. The second class of range-separated functionals, RSH, which includes the range-separated hybrid functionals $\omega$B97X, $\omega$B97XD, and CAM-B3LYP, has two range parameters: $\omega$ to separate the exchange into long- and short-range contributions and a second parameter to separate the short-range exchange into two components (HF and DFT exchange). In comparing the two classes of range-separated functionals, the RSH functionals yield a lower overall MAD than the RS functionals (7.33 kcal mol$^{-1}$ and 10.11 kcal mol$^{-1}$ for the RSH and RS, respectively). As the $\omega$ range separation parameter increases (0.20 ($\omega$B97XD), 0.30 ($\omega$B97X), 0.33 (CAM-B3LYP), 0.40 ($\omega$B97, LC-$\omega$PBE)), the MADs increase (6.52, 7.42, 8.06, 8.74, 11.47 kcal mol$^{-1}$, respectively).

For the entire family of range-separated functionals (both RS and RSH), comparison of the B97-based functionals shows that as the sophistication (i.e., how many ways the exchange energy is separated) of the functional increases ($\omega$B97 < $\omega$B97X < $\omega$B97XD), the deviation of the calculated $\Delta H_f$ values from experiment decreases. This trend in the B97-based functionals for the 4*d* transition metals is counter to the trend observed for first row transition metals, where the performance of the functionals declined as the number of range-separated terms in the functional increased.[19] With the increase in the number of components to describe the exchange energy, the overall percentage of HF exchange to describe the total exchange energy increases. In the study of first row transition metals, nearly half of the molecules examined had possible multi-reference character,[18] which would not benefit from a greater description of the exchange energy by HF. For the second row transition metals in this study, only one molecule had significant multireference character;[23] therefore, increasing the percentage of HF exchange in the description of the exchange energy should yield more accurate results. The further analysis of the range-separated functionals to examine the affect of a dispersion correction is not straightforward, since the value of $\omega$ is not the same for $\omega$97X and $\omega$B97XD, (15.8% and 22.2% HF exchange, respectively); therefore, gauging the importance of the dispersion correction is not recommended.

**3.5. Double-Hybrid Functionals.** Of the functionals included in the study, the two double-hybrid functionals had the lowest overall MADs (mPW2-PLYP, 4.25 kcal mol$^{-1}$ and B2GP-PLYP, 5.19 kcal mol$^{-1}$). Similar conclusions were made for 3*d* transition metals, where the double hybrid functionals (B2-LYP, B2GP-PLYP, and mPW2-PLYP) yielded the smallest deviations from experimental enthalpies of formation.[19] The double functionals have 55% and 65% Hartree−Fock exchange, respectively. In comparison to the single hybrid functional

Table 5. Mean Absolute Deviation, Mean Signed Deviation, Root Mean Square Deviation, and Standard Deviation from Experiment for the TM-4*d* Molecule Set with Optimized Geometries and Enthalpies of Formation Obtained by Each Functional (e.g. BLYP/cc-pVTZ//BLYP/cc-pVQZ)[a]

| functional | MAD | MSD | RMSD | $\sigma$ | functional | MAD | MSD | RMSD | $\sigma$ |
|---|---|---|---|---|---|---|---|---|---|
| BLYP | 17.87 | 13.48 | 28.95 | 21.47 | B1LYP | 15.76 | −15.41 | 22.90 | 15.49 |
| BP86 | 15.90 | 14.35 | 28.53 | 22.47 | M06 | 7.96 | 3.20 | 10.83 | 6.63 |
| PBEPBE | 24.75 | 11.06 | 43.99 | 32.99 | BMK | 11.53 | 0.88 | 14.69 | 8.26 |
| TPSSKCIS | 7.17 | 5.05 | 15.85 | 13.51 | M062X | 9.57 | −7.52 | 12.56 | 7.43 |
| M06-L | 9.87 | 8.25 | 18.84 | 13.98 | $\omega$B97XD | 10.61 | −8.35 | 16.04 | 11.26 |
| B3P86 | 8.89 | 5.24 | 14.85 | 11.24 | $\omega$B97X | 9.31 | 1.25 | 15.67 | 11.37 |
| B3LYP | 8.46 | −4.72 | 11.55 | 7.25 | CAM-B3LYP | 7.85 | −4.11 | 11.11 | 7.30 |
| B971 | 6.27 | 3.00 | 11.08 | 8.66 | $\omega$B97 | 8.79 | −3.67 | 13.52 | 9.64 |
| X3LYP | 9.51 | −5.96 | 14.84 | 10.71 | LC-$\omega$PBE | 11.68 | −2.88 | 15.96 | 10.04 |
| PBE1PBE | 8.44 | −3.97 | 11.76 | 7.59 | mPW2-PLYP | 5.14 | −2.40 | 12.14 | 9.87 |
| mPW1LYP | 20.72 | −20.72 | 29.42 | 19.40 | B2GP-PLYP | 4.95 | −0.92 | 8.38 | 6.39 |

[a]Units are in kcal mol$^{-1}$.

M06-2X, which has a comparable amount of Hartree−Fock exchange with 54%, the inclusion of second-order perturbation theory correlation is noticeable. The M06-2X functional resulted in an MAD of 10.84 kcal mol$^{-1}$. The addition of 25% PT2 correlation energy, with 55% Hartree−Fock exchange, of mPW2-PLYP resulted in an MAD lowering of over 6 kcal mol$^{-1}$. While the different parametrizations of M06-2X and mPW2-PLYP may account for some of the discrepancy, the effect of *ab initio* correlation energy is evident for the second row transition metals. As noted in the original examination of the molecule set with rp-ccCA, the use of a single-reference method does not compromise the theoretically determined enthalpies of formation. This observation is reinforced by examining the effect of double versus single hybridization for density functionals.

**3.6. Geometry Comparison.** The geometries for the complete TM-4*d* set were also optimized for each of the functionals used in combination with the cc-pVTZ-PP basis set. The DFT/cc-pVTZ-PP optimized geometries were compared to the geometries used within rp-ccCA (B3LYP/cc-pVTZ-PP). On average the bond lengths differed by 0.016 Å. Using $ZrO_2$ as a representative example since there are four previous theoretically determined geometries to compare, the Zr−O bond length as determined by B3LYP, B97-1, wB97XD, and mPW2-PLYP was 1.776, 1.770, 1.759, and 1.786 Å, respectively. The O−Zr−O bond angle as determined by the same functionals (B3LYP, B97-1, wB97XD, and mPW2-PLYP) was 108.5°, 108.4°, 109.2°, and 108.1°, respectively. Previous theoretical studies reported the Zr−O bond length as 1.797, 1.780, and 1.806 Å, and the corresponding bond angle as 109.6°, 109.4°, and 108.0°. The optimized geometries obtained with B3LYP and the cc-pVTZ-PP basis set are reported in the Supporting Information. Experimental geometries and previous theoretically determined geometries are included in the Supporting Information.

While the deviations between the B3LYP geometries and the geometries determined by the other functionals included in this study may seem trivial, the impact of the geometries optimized for each functional on the enthalpies of formation ($\Delta H_f$ values) and the overall deviations of the $\Delta H_f$ values from experiment were examined. On average, utilizing the geometry optimized by a functional for the single point energy calculation used to determine the $\Delta H_f$ did not change the MADs and MSDs from experiment. The MAD and MSD, for the $\Delta H_f$ values based upon the DFT-specific optimized structure for each functional are reported in Table 5. The most notable changes in deviations were for two of the GGAs (TPSSKCIS and M06-L). The utilization of the TPSSKCIS and M06-L optimized geometries resulted in a reduction of the MADs for these two functionals by 7 and 2 kcal mol$^{-1}$, respectively.

## 4. CONCLUSION

Overall, the performance of 22 density functionals, including GGAs, HGGAs, HMGGAs, RS, and DHGGAs, in combination with the correlation consistent basis sets and effective core potentials, was examined for the determination of the enthalpy of formation of 30 second row transition metal-containing molecules (TM-4*d* set). Previously, rp-ccCA was used to study the molecule set and a MAD of 2.89 kcal mol$^{-1}$ from experimental enthalpies of formation was observed. The average experimental uncertainty for the set is 3.43 kcal mol$^{-1}$. None of the functionals included in the current study matched the accuracy level of rp-ccCA, though the double hybrid functionals, mPW2-PLYP and B2GP-PLYP, yielded the lowest MADs (4.25 and 5.19 kcal mol$^{-1}$, respectively). The GGA functionals had the largest deviations from experiment and are not recommended for second row transition metal thermochemistry. The HGGAs, specifically those with 20−30% Hartree−Fock exchange, deviated from experiment by, on average, 6−10 kcal mol$^{-1}$, depending on the functional employed. For the range separated functionals, the inclusion of short-range HF exchange did not lower the deviations of the DFT calculated enthalpies of formation from experiment, but it was observed that increasing the value of $\omega$, the range separation parameter, increased the MAD of the range separated functional [0.30 ($\omega$B97X) to 0.33 (CAM-B3LYP) to 0.40 ($\omega$B97, LC-$\omega$PBE), the MADs increase (7.42, 8.06, 8.74, 11.47 kcal mol$^{-1}$, respectively)]. Overall, to obtain the best performance with DFT, the double hybrid functionals, namely mPW2-PLYP, in combination with the cc-pVQZ-PP basis set and ECP should be employed for second row TM thermochemistry.

## ■ ASSOCIATED CONTENT

### Supporting Information

Enthalpies of formation, B3LYP/cc-pVTZ-PP ground state geometries, and comparative geometries from previous experimental and theoretical studies. This material is available free of charge via the Internet at http://pubs.acs.org.


dx.doi.org/10.1021/ct400379z | J. Chem. Theory Comput. XXXX, XXX, XXX−XXX

## AUTHOR INFORMATION


### Corresponding Author

*E-mail: akwilson@unt.edu.


### Notes

The authors declare no competing financial interest.

## ACKNOWLEDGMENTS

This material is based upon work supported by the National Science Foundation under Grant No. CHE-1213874. The authors also thank the National Science Foundation for equipment support via NSF CRIF (CHE-0741936). Additional computing resources were provided by the Academic Computing Services at the University of North Texas. Support from the United States Department of Education for the Center for Advanced Scientific Computing and Modeling (CASCaM) is acknowledged.

## REFERENCES


(1) Hyla-Kryspin, I.; Grimme, S. *Organometallics* **2004**, *23*, 5581.
(2) Quintal, M. M.; Karton, A.; Iron, M. A.; Boese, A. D.; Martin, J. M. L. *J. Phys. Chem. A* **2006**, *110*, 709.
(3) Gutzev, G. A.; Mochena, M. D.; Jena, P.; Bauschlicher, C. W., Jr.; PartridgeIII, H. *J. Chem. Phys.* **2004**, *121*, 6785.
(4) Zhao, Y.; Truhlar, D. G. *Theor. Chem. Acc.* **2008**, *120*, 215.
(5) Zhao, Y.; Truhlar, D. G. *Acc. Chem. Res.* **2008**, *41*, 157.
(6) Yao, C.; Guan, W.; Song, P.; Su, Z. M.; Feng, J. D.; Yan, L. K.; Wu, Z. J. *Theor. Chem. Acc.* **2007**, *117*, 115.
(7) Song, P.; Guan, W.; Yao, C.; Su, Z. M.; Wu, Z. J.; Feng, J. D.; Yan, L. K. *Theor. Chem. Acc.* **2007**, *117*, 407.
(8) Cohen, A. J.; Mori-Sanchez, P.; Yang, W. *Science* **2008**, *321*, 792.
(9) Jensen, F. *Introduction to Computational Chemistry*, 2 ed.; John Wiley and Sons, Ltd.: West Sussex, 2007; p 232.
(10) Cheng, L.; Wang, M. Y.; Wu, Z. J.; Su, Z. M. *J. Comput. Chem.* **2007**, *28*, 2190.
(11) Tekarli, S. M.; Drummond, M. L.; Williams, T. G.; Wilson, A. K. *J. Phys. Chem. A* **2009**, *113*, 8607.
(12) Cundari, T. R.; Leza, H. A. R.; Grimes, T.; Steyl, G.; Waters, A.; Wilson, A. K. *Chem. Phys. Lett.* **2005**, *401*, 58.
(13) Jiang, W.; DeYonker, N. J.; Determan, J. J.; Wilson, A. K. *J. Phys. Chem. A* **2012**, *116*, 870.
(14) Cundari, T. R.; Leza, H. A. R.; Grimes, T.; Steyl, G.; Waters, A.; Wilson, A. K. *Chem. Phys. Lett.* **2007**, *401*, 58.
(15) Housecroft, C. E. *The Heavier d-block Metals: Aspects of Inorganic and Coordination Chemistry*; Oxford Science Publications: Oxford, 1999; p 24.
(16) Levina, A.; McLeod, A.; Seuring, J.; Lay, P. A. *J. Inorg. Biochem.* **2007**, *101*, 1586.
(17) Luo, S.; Truhlar, D. G. *J. Chem. Theory Comput.* **2012**, *8*, 4112.
(18) DeYonker, N. J.; Williams, T. G.; Imel, A. E.; Cundari, T. R.; Wilson, A. K. *J. Chem. Phys.* **2009**, *131*, 024106.
(19) Jiang, W.; Laury, M. L.; Powell, M.; Wilson, A. K. *J. Chem. Theory Comput.* **2012**, *8*, 4102.
(20) DeYonker, N. J.; Peterson, K. A.; Steyl, G.; Wilson, A. K.; Cundari, T. R. *J. Phys. Chem. A* **2007**, *111*, 11269.
(21) Frenking, G.; Antes, I.; Bohme, M.; Dapprich, S.; Ehlers, A. W.; Jones, V.; Neuhaus, A.; Otto, M.; Stegmann, R. *Reviews in Computational Chemistry*; VCH: New York, 1996; Vol. *8*.
(22) Cao, Z.; Dolg, M. *Relativistic Methods for Chemists*; Springer: Berlin, 2009; p 37.
(23) Laury, M. L.; DeYonker, N. J.; Jiang, W.; Wilson, A. K. *J. Chem. Phys.* **2011**, *134*, 214103.
(24) Perdew, J. P.; Schmidt, K. *AIP Conf. Proc.* **2001**, *577*, 1.
(25) Ikeda, A.; Nakao, Y.; Sato, H.; Sakaki, S. *J. Phys. Chem. A* **2007**, *111*, 7124.
(26) Mori-Sanchez, P.; Cohen, A. J.; Yang, W. *J. Chem. Phys.* **2006**, *125*, 201102.
(27) Perdew, J. P.; Zunger, A. *Phys. Rev. B* **1981**, *23*, 5048.
(28) Becke, A. D. *J. Chem. Phys.* **1993**, *98*, 5648.
(29) Grimme, S. *J. Chem. Phys.* **2006**, *124*, 034108.
(30) Schwabe, T.; Grimme, S. *Phys. Chem. Chem. Phys.* **2006**, *8*, 4398.
(31) Yanai, T.; Tew, D.; Handy, N. *Chem. Phys. Lett.* **2004**, *292*, 51.
(32) Chai, J.-D.; Head-Gordon, M. *J. Chem. Phys.* **2008**, *128*, 084106.
(33) Grimme, S. *J. Comput. Chem.* **2006**, *27*, 1787.
(34) Frisch, M. J.; Trucks, G. W.; Schlegel, H. B.; Scuseria, G. E.; Robb, M. A.; Cheeseman, J. R.; Scalmani, G.; Barone, V.; Mennucci, B.; Petersson, G. A.; Nakatsuji, H.; Caricato, M.; Li, X.; Hratchian, H. P.; Izmaylov, A. F.; Bloino, J.; Zheng, G.; Sonnenberg, J. L.; Hada, M.; Ehara, M.; Toyota, K.; Fukuda, R.; Hasegawa, J.; Ishida, M.; Nakajima, T.; Honda, Y.; Kitao, O.; Nakai, H.; Vreven, T.; Montgomery, J. A.; , Jr., Peralta, J. E.; Ogliaro, F.; Bearpark, M.; Heyd, J. J.; Brothers, E.; Kudin, K. N.; Staroverov, V. N.; Keith, T.; Kobayashi, R.; Normand, J.; Raghavachari, K.; Rendell, A.; Burant, J. C.; Iyengar, S. S.; Tomasi, J.; Cossi, M.; Rega, N.; Millam, J. M.; Klene, M.; Knox, J. E.; Cross, J. B.; Bakken, V.; Adamo, C.; Jaramillo, J.; Gomperts, R.; Stratmann, R. E.; Yazyev, O.; Austin, A. J.; Cammi, R.; Pomelli, C.; Ochterski, J. W.; Martin, R. L.; Morokuma, K.; Zakrzewski, V. G.; Voth, G. A.; Salvador, P.; Dannenberg, J. J.; Dapprich, S.; Daniels, A. D.; Farkas, O.; Foresman, J. B.; Ortiz, J. V.; Cioslowski, J.; , and Fox, D. J., *Gaussian 09, Revision B.01*; Gaussian, Inc., Wallingford, CT, 2010.
(35) Peterson, K. A.; Shepler, B. C.; Figgen, D.; Stoll, H. *J. Phys. Chem. A* **2007**, *126*, 124101.
(36) Lee, C.; Yang, W.; Parr, R. G. *Phys. Rev. B* **1988**, *37*, 785.
(37) Miehlich, B.; Savin, A.; Stoll, H.; Preuss, H. *Chem. Phys. Lett.* **1989**, *157*, 2000.
(38) Perdew, J. P. *Phys. Rev. B* **1986**, *33*, 8822.
(39) Toulouse, J.; Savin, A.; Adamo, C. *J. Chem. Phys.* **2002**, *117*, 10465.
(40) Krieger, J. B.; Chen, J. Q.; Kurth, S. *Density Functional Theory and Its Application to Materials*; AIP: New York, 2001; Vol. *577*.
(41) Krieger, J. B.; Chen, J. Q.; Iafrate, G. J.; Savin, A. *Electron Correlations and Materials Properties*; Kluwer Academic: New York, 1999.
(42) Rey, J.; Savin, A. *Int. J. Quantum Chem.* **1998**, *69*, 581.
(43) Tao, J. M.; Perdew, J. P.; Staroverov, V. N.; Scuseria, G. E. *Phys. Rev. Lett.* **2003**, *91*, 146401.
(44) Perdew, J. P.; Burke, K.; Ernzerhof, M. *Phys. Rev. Lett.* **1996**, *77* (18), 3965.
(45) Perdew, J. P.; Burke, K.; Ernzerhof, M. *Phys. Rev. Lett.* **1997**, *78*, 1396.
(46) Zhao, Y.; Truhlar, D. G. *J. Chem. Phys.* **2006**, *125*, 194101.
(47) Hamprecht, F. A.; Cohen, A. J.; Tozer, D. J.; Handy, N. C. *J. Chem. Phys.* **1998**, *109*, 6264.
(48) Adamo, C.; Barone, V. *J. Chem. Phys.* **1999**, *110*, 6158.
(49) Perdew, J. P.; Chevary, J. A.; Vosko, S. H.; Jackson, K. A.; Pederson, M. R.; Singh, D. J.; Fiolhais, C. *Phys. Rev. B* **1992**, *46*, 6671.
(50) Perdew, J. P.; Chevary, J. A.; Vosko, S. H.; Jackson, K. A.; Perderson, M. R.; Singh, D. J.; Fiolhais, C. *Phys. Rev. B* **1993**, *48*, 4978.
(51) Perdew, J. P. *Electronic Structure of Solids*; Akademie Verlag: Berlin, 1991.
(52) Perdew, J. P.; Burke, K.; Wang, Y. *Phys. Rev. B* **1996**, *54*, 16533.
(53) Burke, K.; Perdew, J. P.; Wang, Y. *Electronic Density Funtional Theory: Recent Progress and New Directions*; Plenum: New York, 1998.
(54) Xu, X.; Goddard, W. A., III *Proc. Natl. Acad. Sci. U.S.A.* **2004**, *101*, 2673.
(55) Adamo, C.; Barone, V. *J. Chem. Phys.* **1998**, *108*, 664.
(56) Becke, A. D. *J. Chem. Phys.* **1996**, *104*, 1040.
(57) Boese, A. D.; Martin, J. M. L. *J. Chem. Phys.* **2004**, *121*, 3405.
(58) Chai, J.-D.; Head-Gordon, M. *Phys. Chem. Chem. Phys.* **2008**, *10*, 6615.
(59) Vydrov, O. A.; Scuseria, G. E.; Perdew, J. P. *Chem. Phys.* **2007**, *126*, 154109.
(60) Vydrov, O. A.; Scuseria, G. E. *J. Chem. Phys.* **2006**, *125*, 234109.
(61) Vydrov, O. A.; Heyd, J.; Krukau, A.; Scuseria, G. E. *J. Chem. Phys.* **2006**, *125*, 074106.
(62) Karton, A.; Tarnopolsky, A.; Lame're, J. L.; Schatz, G. C.; Martin, J. M. L. *J. Phys. Chem. A* **2008**, *112*, 12868.

(63) Császár, A. G.; Furtenbacher, T. *Chem.—Eur. J.* **2010**, *16*, 4862.
(64) *Organometallic Thermochemistry Database*; Linstrom, P.J., Mallard, W.G., Eds.; NIST: Gaithersburg, MD, 2005; Vol. *69*.
(65) Laury, M. L.; Boesch, S. E.; Haken, I.; Sinha, P.; Wheeler, R. A.; Wilson, A. K. *J. Comput. Chem.* **2011**, *32*, 2339.
(66) Liu, C.; Peterson, C.; Wilson, A. K. C−O Bond Cleavage of Dimethyl Ether by Transition Metal Ions: A Systematic Study on Catalytic Properties of Metals and Performance of DFT Functionals. *J. Phys. Chem. A* **2013**, *117*, 5140−5148.
(67) Moore, Charlotte E. *Atomic Energy Levels*; National Bureau of Standards: Washington, DC, 1949−1958.